APP Template V1.70 Article id: psab399b Typesetter: MPS Date received by MPS: 09/08/2019 PE: MAC007654 CE: LE:

IOP Publishing Physica Scripta

Phys. Scr. **00** (2019) 000000 (9pp)

Temperature switch and router of two and three-mode noise correlation in Pr^{3+}:YSO crystal

Al Imran[1], Irfan Ahmed[2,3,4], Faizan Raza[1], Yiming Li[1], Abubakkar Khan[1], Habib Ullah[1] and Yanpeng Zhang[1,4]

[1] Key Laboratory for Physical Electronics and Devices of the Ministry of Education and School of Electronic and Information Engineering, Xi'an Jiaotong University, Xi'an 710049, People's Republic of China
[2] Department of Physics, City University of Hong Kong, Hong Kong, People's Republic of China
[3] Department of Electrical Engineering, Sukkur IBA University, 65200, Sindh, Pakistan

E-mail: iahmed8-c@my.cityu.edu.hk and ypzhang@mail.xjtu.edu.cn

Received 11 March 2019, revised 15 July 2019
Accepted for publication 8 August 2019
Published DD MM 2019

Abstract

Rare earth doped crystal Pr^{3+}:Y_2SiO_5 has unique features, whose nonlinear response is dynamically triggered and modulated by the interaction between dressing and phonon effect. In this article, we have demonstrated the switching from two-mode bunching to anti-bunching like phenomenon of noise intensity fluctuations used for noise correlation. Here, switching in bunching phenomenon is caused by relative nonlinear phase, which is induced by self- and cross-phase modulation. In contrast with two-mode bunching, three-mode bunching case hardly follows the switching mechanism attributed to the destructive interaction among the phases of Stokes, anti-Stokes and FL signals. We also have realized switching and routing application in two and three mode bunching. Both functions (switching and routing) are controlled by manipulating temperature of cryostat and gate delay. Our experimental results provide the novel technique for switching and channel equalization ratio of about 96%. The intensity switching speed is achieved about 17 ns.

Keywords: nonlinear optics, four-wave mixing, fluorescence and phonon, routing, swtiching

SQ1 (Some figures may appear in colour only in the online journal)

1. Introduction

In these days, manipulation and detection of correlated and entangled photon pairs are very popular for application of quantum information processing [1–4]. Atomic systems provide a fertile ground to study correlated photon pairs on quantum coherence excitation [5, 6]. However, challenges lying in further integration and miniaturization of quantum photonic devices such as optical quantum computing [7], light coherent storage [8, 9], all optical routing via spontaneous parametric four-wave mixing (SP-FWM) in an atomic ensemble [10]. Recently, solid atom-like media such as rare earth ion Pr^{3+} doped Y_2SiO_5 (Pr^{3+}:YSO) is used to investigate coherent effects due to the long coherence time (0.1–1.0 s) and narrow spectral width (∼MHz) compared with atomic gases [11–13]. Previously, research has accomplished on YSO for optical transmission [14], electromagnetically induced transparency [15], fRequency up-conversion [16]. Also, correlated photon pairs have achieved efficiently from Pr^{3+}: YSO crystal via SP-FWM by using external optical laser source [17]. Intensity-noise correlation and intensity-difference squeezing can be a very promising way to realize entanglement photon pairs and their noise characteristics [18]. It can approach to show about the interference between Stokes, anti-Stokes and FL signals. Consequently, the study on correlation and squeezing can be a potential resource to

[4] Authors to whom any correspondence should be addressed.

know the response of Pr^{3+}: YSO for different application in nonlinear optics.

In this paper, we employ correlated Stokes ($\boldsymbol{E}_S$), anti-Stokes ($\boldsymbol{E}_{AS}$) and fluorescence (FL) to demonstrate two-mode, three-mode bunching. Anti-bunching like phenomenon has been observed with the external dressed state of Pr^{3+}:YSO crystal using temperature of the crystal and the gate delay of the detection system. Bunching has been demonstrated experimentally and theoretically for two-mode and three-mode cases via relative nonlinear phase. Here, we have demonstrated switching of two-mode bunching to anti-bunching like phenomenon by modulating cross- and self-phase using intensive phonon and external gate delay. Also, we have observed that phonon can modulate the relative nonlinear phase by cross-phase modulation (XPM) and gate delay can modulate the relative nonlinear phase by self-phase modulation (SPM). We also realized and proposed method for temperature switching and routing by varying temperature and gate delay.

2. Theoretical model

When laser field $\boldsymbol{E}_1$ is opened, third-order Stokes and anti-Stokes signals are generated along with SP-FWM process, considering the dressing terms and the perturbation chain via $\rho_{00}^{(0)} \xrightarrow{E_1} \rho_{10}^{(1)} \xrightarrow{E_{AS}} \rho_{00}^{(2)} \xrightarrow{E'_1} \rho_{10(S)}^{(3)}$ and $\rho_{00}^{(0)} \xrightarrow{E'_1} \rho_{10}^{(1)} \xrightarrow{E_S} \rho_{00}^{(2)} \xrightarrow{E_1} \rho_{10(AS)}^{(3)}$. Following this perturbation chain and self-dressing effect of $\boldsymbol{E}_1$, one can write the respective third-order nonlinear density matrix elements for the intensity of Stokes and anti-Stokes as

$$\rho_{10(S)}^{(3)} = \frac{-iG_{AS}G_1G'_1}{(\Gamma_{10} + i\Delta_1)(\Gamma_{00} - i\Delta'_1 + |G_1|^2/\Gamma_{00} - i\Delta_1)\Gamma_{11}}, \tag{1}$$

$$\rho_{10(AS)}^{(3)} = \frac{-iG_SG_1G'_1}{(\Gamma_{10} + i\Delta'_1)(\Gamma_{00} - i\Delta_1 + |G_1|^2/\Gamma_{00} - i\Delta_1)\Gamma_{11}}, \tag{2}$$

where, $G_i = -\mu_{ij}E_1/\hbar$ is the Rabi frequency, μ_{ij} is the electric dipole moment between levels $|i\rangle$ and $|j\rangle$, and $\Gamma_{ij} = (\Gamma_i + \Gamma_j)/2$ is the transverse decay rate. Here, i and j represent 0/1. In case of two-level system, lifetime of Stokes or anti-Stokes signal can be written as, $\Gamma_{S/AS} = \Gamma_{00} + \Gamma_{10} + \Gamma_{11}$. The temporal intensity of Stokes/anti-Stokes signal in the two-level system is determined by $I(t) = |\rho_{10(S/AS)}^{(3)}|\exp(-\Gamma_{S/AS}t)$. FL emission intensity is proportional to the square of the diagonal elements of density matrix. The density matrix of the second-order FL via perturbation chain $\rho_{00}^{(0)} \xrightarrow{E_1} \rho_{10}^{(1)} \xrightarrow{E'_1} \rho_{11}^{(2)}$ can be written as

$$\rho_{11}^{(2)} = \frac{-|G_1|^2}{(\Gamma_{10} + i\Delta_1 + |G_1|^2/\Gamma_{00})(\Gamma_{11} + |G_1|^2/(\Gamma_{10} + i\Delta_1))}. \tag{3}$$

Here, $|G_1|^2/(\Gamma_{ij} \pm i\Delta_1)$ is the interaction between dressing and phonon effects of field $\boldsymbol{E}_1$ in equations (1)–(3) [19]. The temporal intensity of FL peak in the two-level system has defined in equation (3), which is determined by $I(t) = |\rho_{11}^{(2)}|\exp(-\Gamma_{FL}t)$, where Γ_{FL} is given by $\Gamma_{FL} = \Gamma_{10} + \Gamma_{11}$. Following the interaction of the coupling field of Pr^{3+}:YSO, the line width broadening of the obtained SP-FWM signal is given by $\Gamma_{ij} = \Gamma_{pop} + \Gamma_{ion\text{-}spin} + \Gamma_{ion-ion} + \Gamma_{phonon} - \Gamma_{dressing}$ [20]. Where, $\Gamma_{pop} = (2\pi T_1)^{-1}$ is the population decay time that depends on the location of the energy levels. The last terms are components of $(2\pi T_2^*)^{-1}$(the reversible transverse relaxation). $\Gamma_{ion\text{-}spin}$ is related to ion-spin coupling effect of the individual ion. $\Gamma_{ion-ion}$ is determined by the interaction among the rare-earth ions and it can either be controlled by the parameter of external field or impurity concentrations. Γ_{phonon} is related to the sample temperature. Whereas, $\Gamma_{dressing}$ is energy levels location, which is induced from the dressing effect. Therefore, Hamiltonian with $G_1 \geqslant \Gamma_{10}$ can be written as the following

$$H = -\hbar\left[\begin{pmatrix} 0 & (G_1/\Gamma_{10}) \\ (G_1^*/\Gamma_{10}) & i\Gamma_{10} + (-1)^i\Delta_1 \end{pmatrix}\right].$$

2.1. Two-mode and three-mode bunching of correlation

Figure 1(b) shows the two-level system of Pr^{3+}:YSO and the laser coupling configuration. The pumping fields $\boldsymbol{E}_1$ (ω_1, Δ_1) with the frequency detuning $\Delta_i = \omega_{mn} - \omega_i$ ($i = 1, 2$) in figure 1(b). Here, ω_{mn} is the corresponding atomic transition frequency between levels $|m\rangle$ and $|n\rangle$, ω_i ($i = 1, 2\ldots$ etc) is the laser frequency. When $\boldsymbol{E}_1$ and $\boldsymbol{E}'_1$ (reflection of $\boldsymbol{E}_1$) are turned on, $\boldsymbol{E}_1$ drives the two-level transition and two narrowband Stokes ($\boldsymbol{E}_S$) and anti-Stokes ($\boldsymbol{E}_{AS}$) signal along with accompanying FL, which are generated under conjugate SP-FWM process with phase matching condition of Stokes and anti-Stokes $\boldsymbol{k}_1 + \boldsymbol{k}'_1 = \boldsymbol{k}_S + \boldsymbol{k}_{AS}$ as depicted in figure 1(a). Where, $\boldsymbol{k}$ and $\boldsymbol{k}'_1$ are wave vectors for $\boldsymbol{E}_1$ and $\boldsymbol{E}'_1$, $\boldsymbol{k}_S$ and $\boldsymbol{k}_{AS}$ wave vectors are output photon pairs. Intensity noise signals of photons are found to be involved in coupling Hamiltonian for propagating through a nonlinear medium, which is given as $H = (\hat{a}_S^+\hat{a}_{AS}^+ + \hat{a}_S\hat{a}_{AS})g/v$. Where, $\hat{a}_S^+\hat{a}_S$ and $\hat{a}_{AS}^+\hat{a}_{AS}$ are the creation and annihilation operators on Stokes and anti-Stokes, respectively, g is the linear or nonlinear gain and v is the group velocity of the photon in the medium. The nonlinear gain is $g = |(-i\omega_{S/AS}\chi_{S/AS}^{(3)}E_1E'_1/2c)|$, where, nonlinear susceptibility is $\chi_{S/AS}^{(3)}$ with phase matching condition, $\omega_{S/AS}$ is the real frequencies generated via Stokes and anti-Stokes; and c is the speed of light. Here, nonlinear susceptibility $\chi_{S/AS}^{(3)} = (N\mu_{S/AS}\rho_{S/AS}^{(3)})/(\varepsilon_0E_1E'_1E_{S/AS})$, where, N is the atomic density of Pr^{3+}:YSO, $\boldsymbol{E}_1$ is the pumping field amplitude, $\rho_{10(S)}^{(3)} = iG_{AS}^*G_1G'_1\exp[i(\boldsymbol{k}_1 + \boldsymbol{k}'_1 - \boldsymbol{k}_{AS}) \cdot \boldsymbol{r}]/[(\Gamma_{10} + i\Delta_1) \times (\Gamma_{00} - i\Delta'_1 + |G_1|^2/\Gamma_{00} - i\Delta_1)\Gamma_{11}]$ is the corresponding density matrix element for Stokes, $\mu_{S/AS}$ is the dipole moments and ε_0 is permittivity.

From the above coupling Hamiltonian, the propagation for Stokes and anti-Stokes signals are given as

$$da_S/dt = ga_{AS}^+\exp(i\phi_S), \tag{4}$$

$$da_{AS}/dt = ga_S^+\exp(i\phi_{AS}), \tag{5}$$

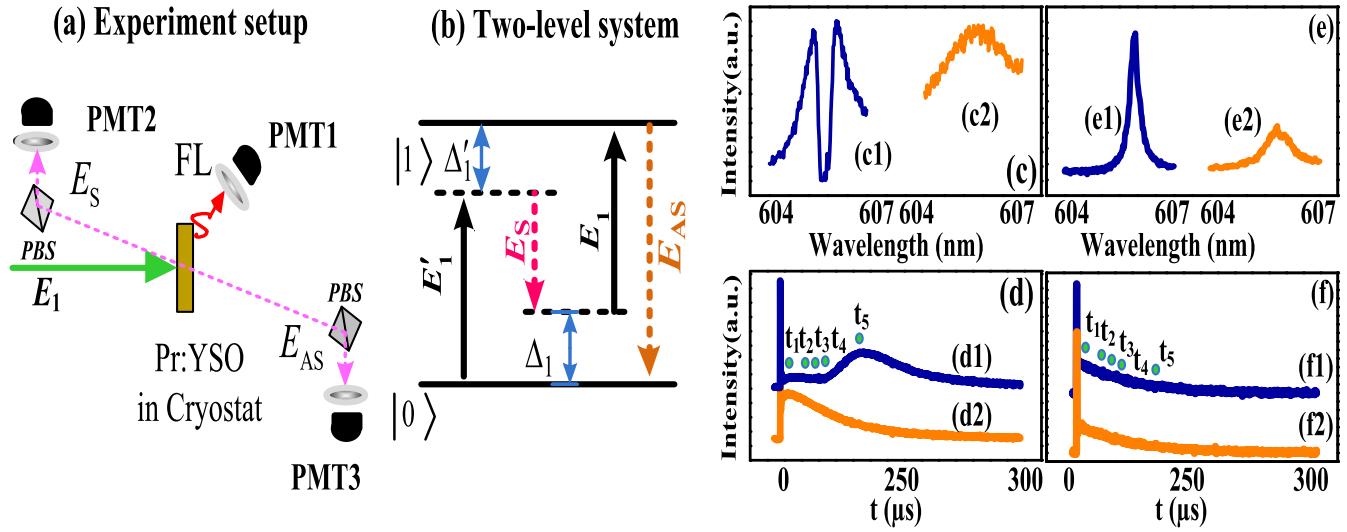

Figure 1. (a) Schematic diagram of experimental setup. (b) Energy levels of two level system in Pr^{3+}:YSO and the laser coupling configuration. (c1)–(c2) Spectral signal for output FL at 77 K and 300 K, respectively. (d1)–(d2) The temporal intensity for FL corresponding to the output spectral signals plotted in (c1)–(c2), respectively. (e1)–(e2) and (f1)–(f2) Spectral and temporal intensities of Stokes at 77 K and 300 K, respectively.

where, ϕ_S and ϕ_{AS} is the induced nonlinear phase through XPM (ϕ_x) and SPM (ϕ_s).ϕ_S and ϕ_{AS} can be derived as

$$\phi_{S/AS} = 2k_{S/AS}[(n_2^s\,|E_{S/AS}|^2 + n_2^x\,|E_1|^2)e^{-r^2}z/n_1^{S/AS},$$

where, $n_1^{S/AS}$ is the linear refractive index of Stokes or anti-Stokes, n_2^s and n_2^x is self- and cross-Kerr nonlinear coefficient. Also, one can write the propagation term of respective density matrix $\rho_i'^{(3)}$ and $\rho_i'^{(1)}$ as

$$\rho_i'^{(3)} = \frac{-iG_i|G_1|^2}{(\Gamma_{10} + i\Delta_1)^2(\Gamma_{00} - i\Delta_1 - i\Delta_1')\Gamma_{11}}, \tag{6}$$

$$\rho_i'^{(1)} = \frac{-iG_i}{(\Gamma_{10} + i\Delta_1 + |G_1|^2/\Gamma_{10})}. \tag{7}$$

Here, $\chi_i'^{(3)} \propto \rho_i'^{(3)}$ and $\chi_i'^{(1)} \propto \rho_i'^{(1)}$ (i represents Stokes/anti-Stokes/FL).

The $N_{S/AS} = \langle \hat{a}_{S/AS}^{+}\,\hat{a}_{S/AS}\rangle$ is the detected number of photons at each PMT (photo multiplier tube in figure 1(a)) and the following intensity $I_{S/AS}(t_{S/AS}) = |N_{S/AS}|\exp(-\Gamma_{S/AS}t_{S/AS})$. So, the responses of the detected intensity of Stokes and anti-Stokes signals in each PMT are proportional to the photon numbers, which are given by

$$\langle \hat{a}_S^{+}\hat{a}_S\rangle = \frac{1}{2}\left[\cos\left(2t\sqrt{AB}\,\sin\frac{\phi_1+\phi_2}{2}\right) + \cosh\left(2t\sqrt{AB}\,\cos\frac{\phi_1+\phi_2}{2}\right)\right]\frac{A}{B}, \tag{8}$$

$$\langle \hat{a}_{AS}^{+}\hat{a}_{AS}\rangle = \frac{1}{2}\left[\cos\left(2t\sqrt{AB}\,\sin\frac{\phi_1+\phi_2}{2}\right) + \cosh\left(2t\sqrt{AB}\,\cos\frac{\phi_1+\phi_2}{2}\right)\right]\frac{B}{A}, \tag{9}$$

where, the substitutions of $\rho_S^{(3)} = Ae^{i\phi_1}$ and $\rho_{AS}^{(3)} = Be^{i\phi 2}$ are taken from equations (1) and (2) ($A(B)$ are the modulus and $\phi_1(\phi_2)$ are the phase angles of $\rho_S^{(3)}(\rho_{AS}^{(3)})$, respectively) and t is time.

The two-mode bunching of intensity correlation between Stokes and anti-Stokes with time delay τ is given by [21, 22]

$$G_{(S,AS)}^{(2)}(\tau) = \frac{\langle \delta\hat{I}_S(t_S)\delta\hat{I}_{AS}(t_{AS}+\tau)\rangle}{\sqrt{\langle[\delta\hat{I}_S(t_S)]^2\rangle\langle[\delta\hat{I}_{AS}(t_{AS}+\tau)]^2\rangle}}\cos(\Delta\phi), \tag{10}$$

where, $\Delta\phi = \phi_S - \phi_{AS} = \Delta\phi_x + \Delta\phi_s$ is relative nonlinear phase between Stokes and anti-Stokes signal based on XPM ($\Delta\phi_x$) and SPM ($\Delta\phi_s$); and $\tau = \tau_S - \tau_{AS}$ is the selected time delay between Stokes and anti-Stokes signal. The two-mode intensity difference squeezing of intensity noise correlated signals are used for two-mode bunching is given by [23, 24]

$$Sq^{(2)} = \mathrm{Log}_{10}\left[\frac{\langle\delta^2(\hat{I}_S - \hat{I}_{AS})\rangle}{\langle\delta^2(\hat{I}_S + \hat{I}_{AS})\rangle}\right]\cos(\Delta\phi). \tag{11}$$

Where, $\langle\delta^2(\hat{I}_S - \hat{I}_{AS})\rangle$ is the mean square deviation of the intensity difference for two-mode bunching and $\langle\delta^2(\hat{I}_S + \hat{I}_{AS})\rangle$ is the mean square deviations of the intensity fluctuations sum for two-mode bunching. Three-mode bunching of intensity noise correlated outputs are given as [20]

$$G^{(3)}(\tau_i, \tau_j, \tau_k) = \frac{\langle\delta\hat{I}_i(\tau_i)\delta\hat{I}_j(\tau_j)\delta\hat{I}_k(\tau_k)\rangle}{\sqrt{\langle\delta\hat{I}_i(\tau_i)^2\rangle\langle\delta\hat{I}_j(\tau_j)^2\rangle\langle\delta\hat{I}_k(\tau_k)^2\rangle}}\cos(\Delta\phi'), \tag{12}$$

where, $i \neq j \neq k(i,\ j$ and k is 1, 2 and 3), $\Delta\phi' = \phi_S - \phi_{AS} - \phi_{FL} = \Delta\phi_x' + \Delta\phi_s'$ is relative nonlinear phase between FL, Stokes and anti-Stokes signal based on XPM and SPM. The intensity-difference squeezing of intensity noise correlated outputs and FL for three-mode bunching

of intensity-noise correlation can be given by [20]

$$Sq^{(3)} = \mathrm{Log}_{10}\left[\frac{\langle\delta^2(\hat{I}_i - \hat{I}_j - \hat{I}_k)\rangle}{\langle\delta^2(\hat{I}_i + \hat{I}_j + \hat{I}_k\rangle}\right]\cos(\Delta\phi'), \qquad (13)$$

where, $\delta^2(\hat{I}_i + \hat{I}_j + \hat{I}_k) = \langle(\hat{I}_i + \hat{I}_j + \hat{I}_k)^2\rangle - \langle\hat{I}_i + \hat{I}_j + \hat{I}_k\rangle^2$ is the mean square deviation of the intensity fluctuations sum for three-mode bunching and $\delta^2(\hat{I}_i - \hat{I}_j - \hat{I}_k) = \langle(\hat{I}_i - \hat{I}_j - \hat{I}_k)^2\rangle - \langle\hat{I}_i - \hat{I}_j - \hat{I}_k\rangle^2$ is the mean square deviation of the intensity difference for three-mode bunching.

3. Experiment setup

Figure 1(a) shows the schematic diagram of the experimental setup along with the detection system. Pr^{3+}:YSO crystal, which is placed in cryostat (CFM-102) to implement our experiment for two-level atomic system. Cryostat container (CFM-102) is used for changing the temperature (K). Also, we have used one tunable dye laser $\boldsymbol{E}_1$ (narrow scan with a 0.04 cm^{-1} line width) pumped by an injection-locked single-mode Nd:YAG laser (Continuum Powerlite DLS 9010, 10 Hz repetition rate, 5 ns pulse width). The generated FL intensity, noise intensities of Stokes and anti-Stokes signals are reflected by beam splitter; and the reflected signals are detected in photomultiplier tubes (PMTs). In our experiment setup, we have placed one near PMT1 and two far PMTs (PMT2 and PMT3) at 13 cm and 118 cm, respectively, from the cryostat container. FL signal is obtained at PMT1. Stokes and anti-Stokes signal is obtained at PMT2 and PMT3. Stokes, anti-Stokes and FL signals are investigated in Pr^{3+}: YSO crystal. Temporal output signals are obtained by the digital oscilloscope and spectral signals are recorded by PMT. The graphical representations of the spectral and temporal intensities are shown in figures 1(c)–(f). Positioning of gate delays t_1–t_5 (μs) are marked on the temporal intensity of the output signal in figures 1(d1) and (f1). In case of Stokes and anti-Stokes signals, two-mode bunching of intensity noise-correlation is recorded between PMT2 and PMT3 for SP-FWM process. We employ FL intensity, and intensities of Stokes and anti-Stokes for two-mode bunching and three-mode bunching correlation in two ways. Firstly, we investigate two-mode and three-mode bunching via relative nonlinear phase. Secondly, using these intensities (FL, Stokes and anti-Stokes), squeezing is calculated by subtraction and addition among the signals analyzed with a spectrum analyzer between relative noise intensity difference and sum as indicated in equations (11) and (13).

At high temperature 300 K, the phonon effect (Γ_{phonon}) is increased due to increase in temperature and phonon relating with $\Gamma_{ij} = \Gamma_{\mathrm{pop}} + \Gamma_{\mathrm{ion\text{-}spin}} + \Gamma_{\mathrm{ion-ion}} + \Gamma_{\mathrm{phonon}} - \Gamma_{\mathrm{dressing}}$ and Γ_{10}. So, Γ_{10} can be decreased at 77 K. Spectral signal ($\rho_{11}^{(2)}$ in equation (3)) characterizes FL with AT-splitting due to increase of dressing effect ($|G_1|^2/(\Gamma_{10} + i\Delta_1)$) in figure 1(c1) at temperature 77 K. At 300 K, AT-splitting is not obtained in FL signal due to decrease of dressing effect $|G_1|^2/(\Gamma_{10} + i\Delta_1)$ in figure 1(c2). Temporal signal of FL $I(t) = |\rho_{11}^{(2)}|\exp(-\Gamma_{\mathrm{FL}}t)$ is shown in figures 1(d1)–(d2) at 77 K and 300 K, respectively. Changing of temperature from 77 to 300 K, temporal signal splitting in figure 1(d1) is vanished in figure 1(d2) due to decrease of dressing effect $|G_1|^2/\Gamma_{10}$, since Γ_{10} is increased with temperature. From the above Hamiltonian, here one can say that the splitting value of dressed state level $\lambda_\pm = [(-1)^i\Delta_1 + i\Gamma_{10} \pm \sqrt{\Delta_1^2 + 4|G_1|^2/\Gamma_{10} + 2i\Delta_1\Gamma_{10} - (\Gamma_{10})^2}]/2$ is decreased due to the phonon broadening effect. While, temporal $I(t) = |\rho_{10(S)}^{(3)}|\exp(-\Gamma_S t)$ and spectral of Stokes signal ($\rho_{10(S)}^{(3)}$ in equation (1)) are shown in figures 1(f1)–(f2) and figures 1(e1)–(e2) at temperature 77 K and 300 K, respectively. When temperature will change from 77 K to 300 K, linewidths of spectral FL ($\rho_{11}^{(2)}$ in equation (3)) and Stokes signal ($\rho_{10(S)}^{(3)}$ in equation (1)) are increased due to increase of Γ_{10}, Γ_{11} in equation (3), and Γ_{00}, Γ_{10}, Γ_{11} in equation (1), respectively. According to the Spectral and temporal signal of Stokes, one can obtain almost same signal for anti-Stokes likewise Stokes. So, the temperature can effect on the nonlinear phase (ϕ_S and ϕ_{AS}) of spectral signals and output photon beams $\langle\hat{a}_{S/AS}^+\hat{a}_{S/AS}\rangle$ which can change the relative nonlinear phase of the two- and three-mode bunching of intensity noise-correlation $G_{(S,AS)}^{(2)}(\tau)$ in figure 2. Also, by changing of temperature from 77 to 300 K, lifetime of Γ_S in figure 1(f1) is decreased in figure 1(f2).

4. Results and discussion

Figures 2(a1)–(a4) shows the obtained two-mode bunching and anti-bunching like phenomenon of second-order intensity noise correlation at different temperatures 240 K, 160 K, 100 K and 77 K, respectively. Here in figures 2(a1)–(a4), two-mode bunching signal is obtained from output Stokes and anti-Stokes signals by exciting the laser beam $\boldsymbol{E}_1$ at wavelength 605.9 nm for two-level system in YSO crystal. The temperature dependent output intensities are also recorded by varying the temperature of YSO crystal at 240 K, 160 K, 100 K and 77 K via cryostat container. Two-mode bunching of intensity-noise correlation can be obtained by substituting their temporal intensities into equation (10). Two-mode bunching with decreasing trend of temperature is shown in figures 2(a1)–(a4). When temperature is fixed at 240 K in figure 2(a1), the amplitude of two-mode bunching between Stokes and anti-Stokes signal $G_{S/AS}^{(2)}(\tau)$ from equation (10) obtains positive (0.86 at delay time ($\tau = 0$)) and waveform of correlation curve is broad. Two-mode bunching of intensity-noise correlation $G_{S/AS}^{(2)}(\tau)$ between Stokes and anti-Stokes in equation (10) is obtained from intensity output photons $\langle\hat{a}_{S/AS}^+\hat{a}_{S/AS}\rangle$ in equations (8), (9). According to the temperature effect on $G_{S/AS}^{(2)}(\tau)$, coherence time of $\langle\hat{a}_{S/AS}^+\hat{a}_{S/AS}\rangle$ decreases at high temperature, which causes the modulus of $A(B)$ to become broad in equations (8), (9). So, the amplitude of two-mode bunching signal $G_{S/AS}^{(2)}(\tau)$ becomes broad at temperature 240 K. When temperature is decreased to 77 K, the amplitude of the two-mode bunching is changed from 0.86 to −0.8. This negative value of bunching is termed as anti-bunching like phenomenon. The switching from two-mode bunching to anti-bunching like phenomenon occurs at 100 and 77 K as shown in

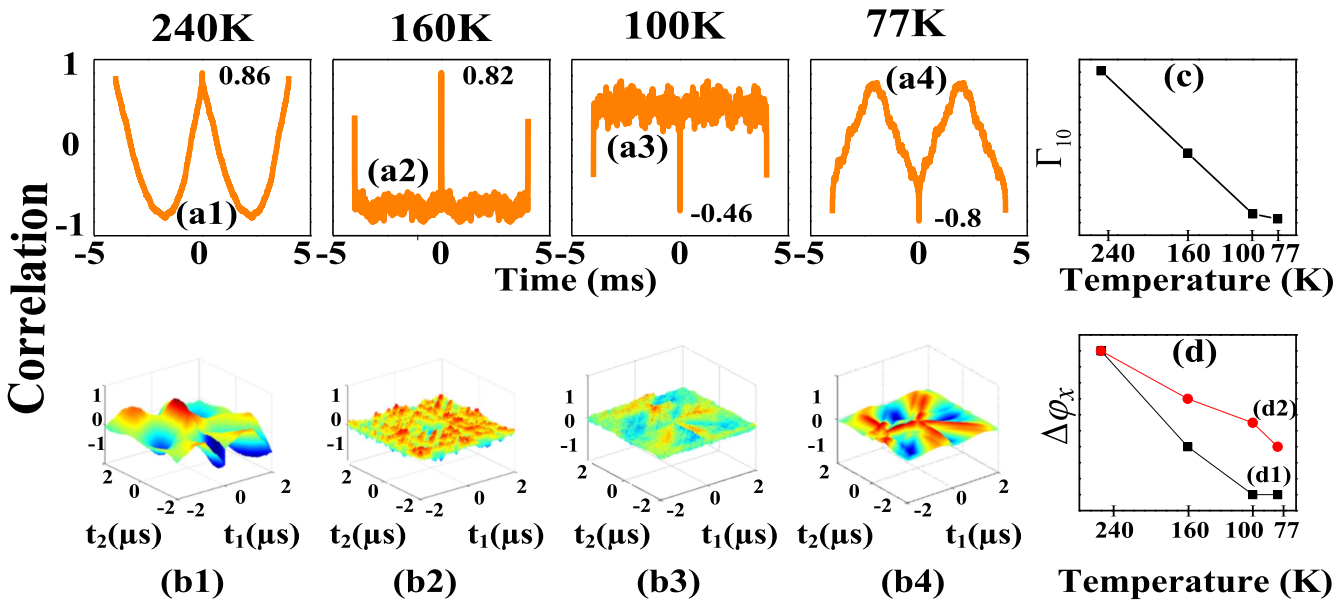

Figure 2. (a1)–(a4) Shows two-mode bunching and anti-bunching like phenomenon from output Stokes and anti-Stokes for two-level system of Pr^{3+}:YSO crystal with laser beam $\boldsymbol{E_1}$ wavelength 605.9 nm at different temperatures 240 K, 160 K, 100 K and 77 K, respectively. (b1)–(b4) shows three-mode bunching calculated from output Stokes, anti-Stokes and FL with experimental condition defined for (a1)–(a4), respectively. (c) Dependent curve of Γ_{10} versus temperature. (d1)–(d2) Dependent curves of $\Delta\phi_x$ versus temperature, where (d1) is for two-mode bunching and (d2) is for three-mode bunching.

figures 2(a3)–(a4). This switching of two-mode bunching to anti-bunching like phenomenon can be explained by the temperature dependent phonon term Γ_{10} from the density matrix element $\rho_{10}^{(3)}$ in equations (1) and (2), and their propagation terms described in equations (6) and (7). At high temperature, the phonon effect is increased due to increase of temperature. Since the Γ_{10} lies in the denominator in density matrix element equations, enhanced Γ_{10} decreases the density matrix element and propagation term at high temperature (likewise in figure 2(e2)). Also, the density matrix elements and propagation terms decreases the nonlinear gain for $\chi'^{(3)}_{S/AS}$. Linear susceptibility $\chi'^{(1)}_{S/AS}$ and nonlinear susceptibility $\chi'^{(3)}_{S/AS}$ are proportional to the propagation term and density matrix element as described in theoretical model. With reducing nonlinear gain, the results are observed as two-mode bunching of Stokes and anti-Stokes in figures 2(a1), (a2). When the temperature is decreased to 100 and 77 K, phonon effect Γ_{10} decreases and dressing effect increases significantly along with propagation terms (likewise figure 1(e2)). Relationship between Γ_{10} versus temperature is shown in figure 2(c) by using a dependent curve. In principles, the enhanced gain has strong bunching at low temperature 77 K but in negative order. This switching of two-mode bunching to anti-bunching like phenomenon can be also explained from linear refractive index and linear gain in Kerr medium. As linear and nonlinear susceptibility ($\chi'^{(1)}_{S/AS}$ and $\chi'^{(3)}_{S/AS}$) are proportional to density matrix element $\rho'^{(1)}_{S/AS}$ and $\rho'^{(3)}_{S/AS}$, the $\rho'^{(1)}_{S/AS}$ and $\rho'^{(3)}_{S/AS}$ can modulate the linear refractive index and cross-Kerr nonlinear coefficients $n_1^{S/AS}$ and $n_2^{S/AS}$ that results from the XPM. Owing to this, relative nonlinear phase $\Delta\phi_x = \phi_S - \phi_{AS} = 2(k_S n_2^S - k_{AS} n_2^{AS})|E_1|^2 e^{-r^2} z/n_1^{S/AS}$ between $\boldsymbol{E}_S$ and $\boldsymbol{E}_{AS}$ signal is significantly modulated. Where, $n_1^{S/AS} = \sqrt{1 + Re(\chi'^{(1)}_{S/AS})}$ is linear refractive index for Stokes and anti-Stokes field, $n_2^{S/AS}$ is cross-Kerr nonlinear coefficient (i represents Stokes or anti-Stokes), r is the radius of Gaussian incident beam from laser and z is the length of the YSO crystal's lens (z = 3 mm). Here, ϕ_S and ϕ_{AS} are the nonlinear phase induced on the output Stokes and anti-Stokes signals. Therefore, $n_1^{S/AS}$ is increased as per the definition of nonlinear and linear refractive index at low temperature 77 K. Enhancing $n_1^{S/AS}$ does not only increasing the intensity of Stokes and anti-Stokes signal but also decreases the nonlinear phase $\Delta\phi_x$. When temperature is changed to 100 and 77 K, intensity of FL signal is increased and $\Delta\phi_x$ is also changed from 0 to $-\pi$ as demonstrated in figures 2(a3)–(a4). Relationship between $\Delta\phi_x$ versus temperature is shown in figure 2(d1) for two-mode bunching. The measured two-mode bunching suggests that the correlated output has negative amplitude due to the factor of cos($\Delta\phi$) in equation (10). In figure 2(a4), broad waveform is obtained, which is similar to two-mode bunching obtained at 300 K shown in figure 2(a1). Also, sharp waveform of two-mode bunching obtained at 160 and 100 K in figures 2(a2), (a3). One can say that two-mode bunching is switched to anti-bunching like phenomenon due to interaction between phonon and dressing at different temperature.

Figures 2(b1)–(b4) shows the measured three-mode bunching of third-order correlation. which are plotted by recording and substituting temporal intensities of FL, Stokes and anti-Stokes signals in equation (12). When temperature is fixed at 240 K, three-mode bunching is observed as shown in figure 2(b1). At this temperature, phonon term Γ_{10} increases in equations (1)–(3) and dressing field decreases in propagation terms of equations (6) and (7). The propagation term $\rho'^{(1)}_{S/AS/FL}$ reduces the linear susceptibility $\chi'^{(1)}_{S/AS/FL}$. When

temperature (K) is reduced to 77 K, multiple peaks of three-mode bunching are gradually reduced in figures 2(b1)–(b4). This gradual decrease in the peak of three-mode bunching can be explained from interaction between phonon Γ_{10} and dressing effect in Stokes, anti-Stokes and FL signal. As temperature is decreased to 77 K, the FL starts to split and AT-splitting in both spectral ($\rho_{11}^{(2)}$ in equation (3)) and temporal signals are obtained by dressing effect as demonstrated in figures 1(c1) and (d1), respectively. Besides, linewidth of intensity of Stokes and anti-Stokes signals ($\rho_{10(S/AS)}^{(3)}$ in equations (1), (2)) can be also decreased (likewise figure 1(c1)). So, the nonlinear phase (ϕ_S, ϕ_{AS} and ϕ_{FL}) of output photon beams of Stokes, anti-Stokes and FL ($\langle \hat{a}_{S/AS/FL}^{+} \hat{a}_{S/AS/FL} \rangle$) are decreased with reducing temperature along with the phase modulation by linear refractive index $n_1^{S/AS/FL}$ as defined in figures 2(a3), (a4). This $n_1^{S/AS/FL}$ also acts on the FL. So, the combined relative nonlinear phase is induced by XPM on the FL, Stokes and anti-Stokes which can be given as

$$\Delta\phi'_x = \phi_S - \phi_{AS} - \phi_{FL} = 2(k_S n_2^S - k_{AS} n_2^{AS} + k_{FL} n_2^{FL})|E_l|^2 e^{-r^2} z / n_1^{S/AS/FL}.$$

The three-mode bunching in figures 2(b1)–(b4), where $\Delta\phi'_x$ is changed from 0 to $-\pi/3$. Relationship between $\Delta\phi'_x$ versus temperature is shown in figure 2(d2) for three-mode bunching.

The temperature switch is realized by the two-mode bunching of intensity noise correlation signals, whose results observed in figures 2(a1)–(a4). Our experiment result defined the switching contrast as $C = (I_{min} - I_{max})/(I_{min} + I_{max})$, where I_{min} and I_{max} are the minimum and maximum value of intensities, respectively. In our experiment, switching contrast C changes from 90% (figure 2(a1)) to 70% (figure 2(a4)) as temperature of cryostat is decreased from 300 to 77 K. The $\boldsymbol{E}_l$ field is controlled by electro-optical modulator, and its speed about 10 ns. The switching speed is controlled by the atomic coherence time. The total switching speed (20 ns) is taken to be the quadrature sum of several independent contributions. Router application is realized from three-mode bunching of intensity noise correlation results observed in figure 3(b). Channel equalization ratio $P = 1 - \sqrt{\sum_1^{1-N}(a_i - a)^2}/a$ is used to measure the de-multiplexing effect, where a is the area of one peak and a_i is the area of each peak or gap between peaks, and N is the total number of peaks after conversion. From our experiment, channel equalization P can decrease from 95% (figure 3(b1)) to 78% (figure 3(b4)) as temperature is changed from 240 to 77 K. Channel contrast can be defined as $S = (t - t')/(t + t')$, then maximum contrast is observed in figure 2(b1) i.e. $S = 90\%$, greater channel contrast will result in greater accuracy of information from figure 2(b1).

Figures 3(a1)–(a3) shows three-mode bunching of third-order noise correlation of output FL, Stokes and anti-Stokes signal calculated by equation (12). The output intensities are obtained from Pr^{3+}:YSO crystal at temperature of 120 K with different gate delays (μs). The two-level system is excited by $\boldsymbol{E_1}$ at 605.9 nm. At gate delay 20 μs (t_1 marks in figures 1(d1) and (f1)), the observed waveform of bunching is found to be broad with positive amplitude in figure 3(a1). When gate delay t_1 (μs) is changed to 60 μs (t_2 marks in figures 1(d1) and (f1)), the multiple peaks of three-mode bunching are reduced to single peak as shown in figure 3(a2). When gate delay is at 150 μs (t_4 marks in figures 1(d1) and (f1)), the resultant three-mode bunching in figure 3(a3) is found to have less amplitude than correlation curve shown in figure 3(a2). This phenomenon can be further explained in temporal signals of Stokes, anti-Stokes and FL where changing gate delay. When increasing gate delay at a fixed temperature 120 K, intensities are changed in temporal signals of FL, Stokes and anti-Stokes. So, nonlinear phase (ϕ_S, ϕ_{AS} and ϕ_{FL}) of output photon beams ($\langle \hat{a}_{S/AS/FL}^{+} \hat{a}_{S/AS/FL} \rangle$) changed with increasing of gate delay. But here, contribution of ϕ_S and ϕ_{AS} is same. So, ϕ_S and ϕ_{AS} are balanced with each other and only ϕ_{FL} can change the relative nonlinear phase. For this reason, peak of three-mode bunching is gradually reduced. Here, relative nonlinear phase is induced by SPM

$$\Delta\phi'_s = \phi_S - \phi_{AS} - \phi_{FL} = 2(k_S |E_S|^2 n_2^S - k_{AS} |E_{AS}|^2 n_2^{AS} - k_{FL} |E_{FL}|^2 n_2^{FL}) e^{-r^2} z / n_1^{S/AS/FL}.$$

Here in figure 3(a3), anti-bunching-like phenomenon is not dramatically changed. So, $\Delta\phi'_s$ is assumed to change from 0 to $-\pi/3$ in figure 3(a3). Relationship between $\Delta\phi_s$ versus gate delay (μs) is shown in figure 3(d) by using a dependent curve for three-mode bunching. Figures 3(b1)–(b3) shows intensity difference squeezing result corresponding to three-mode bunching shown in figures 3(a1)–(a3). The same intensity outputs are used at defined gate delays in equation (13) to calculate the three mode intensity difference squeezing. The intensity difference $\delta^2(\hat{I}_{FL} - \hat{I}_S - \hat{I}_{AS})$ is demonstrated by red curves in figures 3(b1)–(b3), whereas the intensity noise sum $\delta^2(\hat{I}_{FL} + \hat{I}_S + \hat{I}_{AS})$ is plotted as black curves in figures 3(b1)–(b3). In figure 3(b1), squeezing difference between intensity difference and intensity sum is found to be -7.94 dB at 20 μs gate delay. When gate delay is changing from 20 μs to 150 μs in figures 3(b1)–(b3), squeezing difference is gradually decreasing from -7.94 to -1.02 dB. This reduction in the squeezing is corresponded to the changing of intensity of output photon beams $\langle \hat{a}_{S/AS/FL}^{+} \hat{a}_{S/AS/FL} \rangle$, which are caused by the increased gate delays. Therefore, the outputs of FL, Stokes and anti-Stokes signals are found to be decreased at gate delays of 20, 60 and 150 μs. When two level system is excited by input beam $\boldsymbol{E_1}$ of wavelength 609.2 nm. Comparing with different excitation wavelengths (605.9 and 609.2 nm), the three-mode bunching is observed stronger with 609.2 nm in figures 3(c1)–(c3). This is due to resonant excitation of Pr^{3+}:YSO at wavelength of 609.2 nm.

In figures 3(a1)–(a3), when gate position is set at to 150 μs, five channels are successfully converted into single channel and channel equalization ratio (P) decreases from 96% (figure 3(a1)) to 20% (figure 3(a3)) and channel contrast reduces to $\eta = 25\%$ (figure 3(a3)) contrast.

Here in figures 4(a1)–(a4), we have measured two-mode bunching by changing gate delay from 20 to 200 μs (t_1–t_4

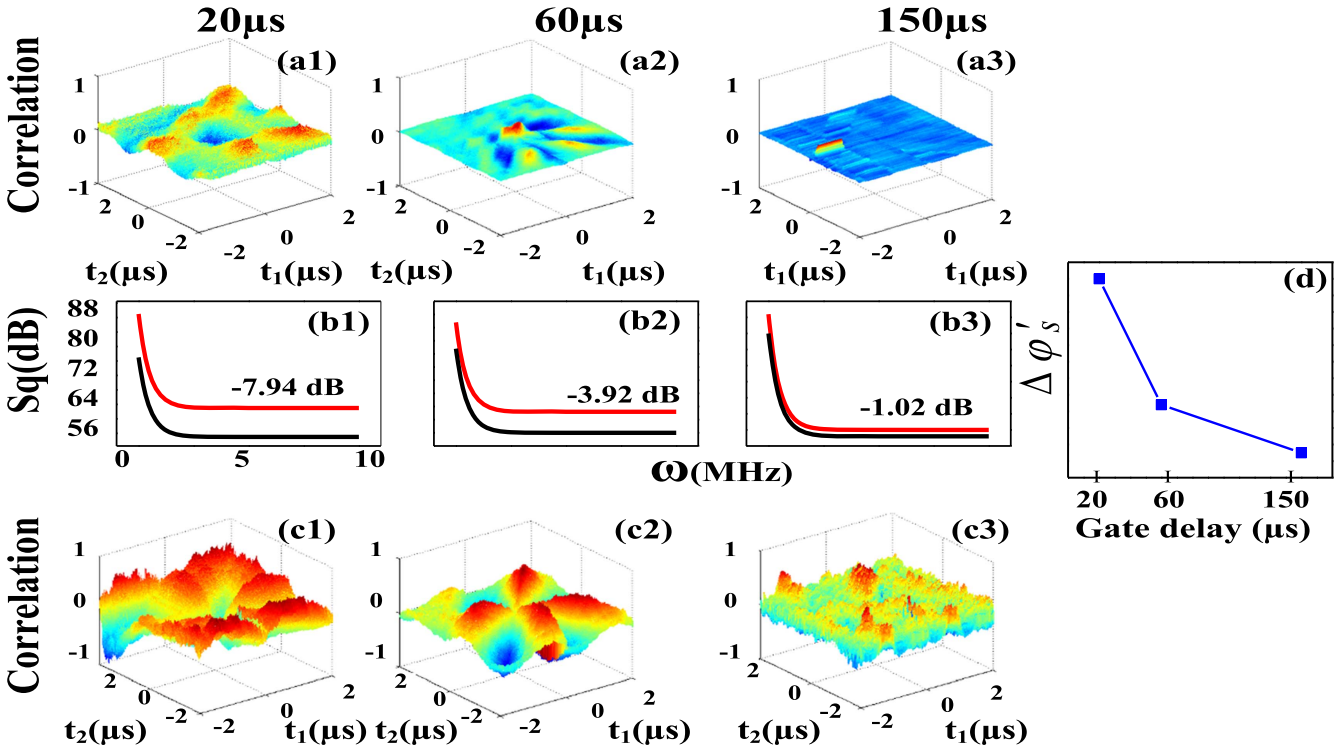

Figure 3. (a1)–(a3) Three-mode bunching with different gate delays of 20, 60 and 150 μs, excited by $\boldsymbol{E}_1$ with 605.9 nm at a fixed temperature of 120 K. (b1)–(b3) shows intensity difference squeezing corresponding to (a1)–(a3), respectively. (c1)–(c3) shows same as (a1)–(a3) respectively, but with excitation source of $\boldsymbol{E}_1$ at 609.2 nm. (d) Dependent curve of $\Delta\phi'_s$ versus gate delay for three-mode bunching (a1)–(a3) and (c1)–(c3).

mark in figures 1(d1) and (f1). For measuring two-mode bunching, we blocked the PMT3 and kept the rest of the PMTs on scanning mode. Here, the two-level system is excited by input beam of wavelength 605.9 nm and emitted signals are plotted using

$$G^{(2)}_{(\mathrm{FL},S)}(\tau) = \frac{\langle \delta\hat{I}_{\mathrm{FL}}(t_{\mathrm{FL}})\delta\hat{I}_{\mathrm{S}}(t_{\mathrm{S}}+\tau)\rangle}{\sqrt{\langle[\delta\hat{I}_{\mathrm{FL}}(t_{\mathrm{FL}})]^2\rangle\langle[\delta\hat{I}_{\mathrm{S}}(t_{\mathrm{S}}+\tau)]^2\rangle}}\cos(\Delta\phi),$$

where, $\tau = \tau_{\mathrm{FL}} - \tau_{\mathrm{S}}$. When gate delay t_1 is fixed at 20 μs, the waveform of measured bunching is broad and the measured amplitude is 0.72 shown in figure 4(a1). When the gate delay is changed to 60 and 100 μs, the amplitude of two-mode bunching is gradually decreased from 0.72 to 0.65 in figure 4(a3). At this gate delay, similar phenomenon of bunching appears in case of three-mode bunching in figure (3). Since, the intensity of Stokes and FL in temporal signal are decreasing with increasing of gate delay (gate delay marks in figures 1(d1) and (f1)), the amplitude of two-mode bunching is also observed to be reduced in figures 4(a2)–(a4). When gate delay is fixed at 200 μs (t_5 marks in figures 1(d1) and (f1)), bunching is switched to anti-bunching like phenomenon and amplitude is about -0.9 as illustrated in figure 4(a4). One may consider that switching obtained here is due to interaction between Stokes, and FL signal at gate delay 200 μs. When gate delay is at position t_5 in both figures 1(d1) and (f1), the difference between positive peak of FL and flat peak of Stokes can change the relative nonlinear phase of two-mode bunching. Also, gate delay can change the nonlinear phase (ϕ_{FL} and ϕ_{S}) of output photon beams $\langle\hat{a}^{+}_{\mathrm{S/FL}}\hat{a}_{\mathrm{S/FL}}\rangle$, which can change also the relative nonlinear phase of the two-mode bunching of intensity noise-correlation $G^{(2)}_{(\mathrm{FL},S)}(\tau)$. Here, relative nonlinear phase is induced by SPM $\Delta\phi_s = \phi_{\mathrm{FL}} - \phi_{\mathrm{S}} = 2(k_{\mathrm{FL}}|E_{\mathrm{FL}}|^2 n_2^{\mathrm{FL}} - k_{\mathrm{S}}|E_{\mathrm{S}}|^2 n_2^{\mathrm{S}})\mathrm{e}^{-r^2}z/n_1^{\mathrm{FL/S}}$. Since two-mode bunching is switched to anti-bunching —like phenomenon, $\Delta\phi_s$ is changed from 0 to $-\pi$ in figure 4(a4). Dependent curve for figures 4(a1)–(a4) and (b1)–(b4) is demonstrated to illustrate the relationship between $\Delta\phi_s$ versus gate delay in figure 4(e1). SPM can be ignored at nearby gate delay on $\boldsymbol{E}_{\mathrm{FL}}$ and $\boldsymbol{E}_{\mathrm{AS}}$. Therefore, the relative phase between FL and Stokes is same as at initial gate delays. This same phenomenon is applied to figures 4(b1)–(b4) at 300 K. Amplitude of correlation curves observe in figures 4(b1)–(b4), which are sharp as compare to correlation curves presented in figures 4(a1)–(a4). When temperature is increased, Γ_{10} is increased and it makes sharp waveform of obtained bunching signal at 300 K in figures 4(b3)–(b4). When temperature of cryostat is fixed at 120 K, two-mode bunching of intensity-noise correlation between stokes and anti-Stokes is observed in two-level system by varying gate delay in figures 4(c1), (c2)–(c3). Relationship between Γ_{10} versus gate delay is shown in figure 4(d2) at 120 K by using a dependent curve. By changing gate delay from 20 to 150 μs (t_1–t_4 marks in figure 1(f)), amplitude of two-mode bunching decreases and it can be explained from relative nonlinear phase change induced by SPM. In figures 4(c1)–(c3), bunching to anti-bunching like phenomenon is not observed as gate delay changed in small range (up to 150 μs) when

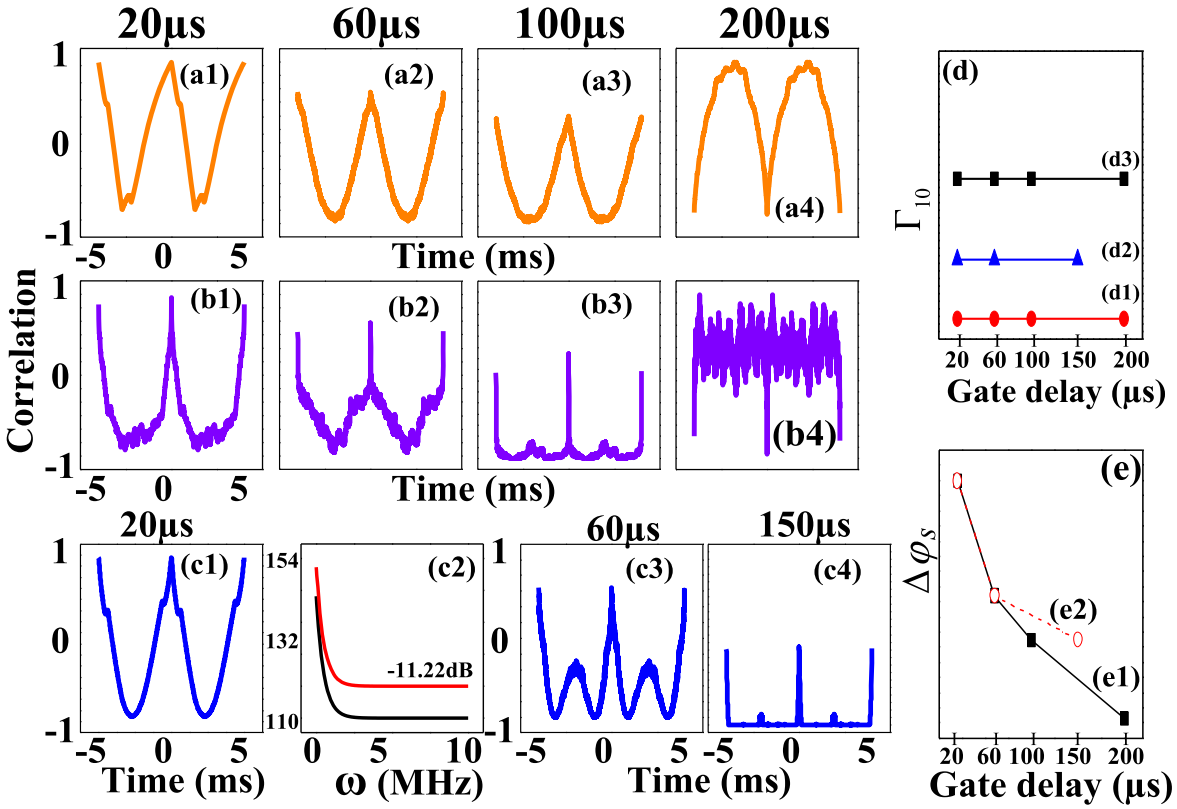

Figure 4. (a1)–(a4) and (b1)–(b4) Show the two-mode bunching between FL and Stokes at gate delay of 20 μs, 60 μs, 150 μs and 200 μs at crystal temperature of 77 K and 300 K, respectively. (c1) and (c3)–(c4) Shows two-mode bunching between Stokes and anti-Stokes at 120 K with different gate delay 20, 60 and 150 μs. (c2) Shows intensity difference squeezing results corresponding (c1). (d) Dependent curve of Γ_{10} versus gate delay, where (d1), (d2) and (d3) are for 77 K, 120 K and 300 K, respectively. (e) Dependent curve of $\Delta\phi_s$ versus gate delay, where (e1) is for (a1)–(a4) and (b1)–(b4), and (e2) is for (c1) and (c3)–(c4), respectively.

compared to figures 4(a1)–(a4) and (b1)–(b4). However, in figures 4(c1)–(c3) waveforms of correlation curves follow similar behavior as discussed in figures 4(a1)–(a4) and (b1)–(b4). Here, relative phase change is induced by SPM in figures 4(c1)–(c4) and $\Delta\phi_s = \phi_S - \phi_{AS} = 2(k_S|E_S|^2 n_2^S - k_{AS}|E_{AS}|^2 n_2^{AS})e^{-r^2}z/n_1^{S/AS}$. At 150 μs gate delay in figure 4(c4), two-mode bunching is not followed to anti-bunching-like phenomenon. So, $\Delta\phi_s$ is predicted to be changed from 0 to $-\pi/3$ in figure 4(c4). Here, intensity of temporal signals of Stokes and anti-Stokes in figure 1(f) are changed with increasing of gate delay (μs). Also, contribution of ϕ_S and ϕ_{AS} is equal in $\Delta\phi_s$. But, the relative nonlinear phase $\Delta\phi_s$ can be changed with the help of increasing linear refractive index $n_1^{S/AS}$ for self-dressing effect of $|G_{S/AS}|^2$. Relationship between $\Delta\phi_s$ versus gate delay is shown in figure 4(e2) by using dependent curve for figures 4(c1), (c3) and (c4). This result in decreasing amplitude of two-mode bunching is observed in figure 4(c4). The intensity difference $\delta^2(\hat{I}_S - \hat{I}_{AS})$ is demonstrated by red curve in figure 4(c2), whereas the noise sum $\delta^2(\hat{I}_S + \hat{I}_{AS})$ is shown using black curve in figure 4(c2). Here in figure 4(c2), intensity difference squeezing is almost -11.22 dB at gate delay 20 μs.

The switching phenomenon of two-mode bunching to anti-bunching like phenomenon could be used to realize an optical transistor as a switch model. One can easily predict that if the intensity of correlation is negative (figures 4(a4) and (b4)), the two-mode bunching switch will remain in the OFF state. When the intensity of the bunching signal is positive (figures 4(a1) and (b1)), then the switch will remain in ON state. The switching contrast calculated is about $C = 120\%$ (figures 4(a1) and (a4)).

5. Conclusion

We have investigated two-and three-mode bunching of intensity noise correlated signals of Pr^{3+}:Y_2SiO_5 crystal by changing temperature and gate delay. The results show that two-mode bunching with broad and sharp waveform, and it can switch to anti-bunching like phenomenon due to the interaction between phonon and dressing effect. Phonon changes the nonlinear relative phase of correlated signals employed to bunching by cross- and SPM. The nonlinear relative phase obtained through such modulation switches the two-mode bunching from 0 to $-\pi$. For three-mode bunching, the nonlinear phase changes the phase shift from 0 to $-\pi/3$. The temperature switch was realized by the switching of bunching due to a nonlinear phase induced by SPM and XPM. Moreover, optimized switching contrast was perceived for switching applications by using correlation in contrast to the intensity signal. Channel equalization ratio and contrast index is controlled by gate delay and temperature of cryostat.

Atom-like nonlinear crystal leads to interaction between phonon and dressing. Since temperature switch and routing application has been realized in Pr^{3+}:YSO crystal, it can be obtained also in other nonlinear crystal such as NV center, europium (Eu^{3+}) doped YPO_4, Praseodymium (Pr^{3+}) doped YPO_4 etc.

Acknowledgments

This work was supported by the National Key R&D Program of China (2017YFA0303700, 2018YFA0307500), National Natural Science Foundation of China (11804267, 61605154, 11604256).

ORCID iDs

Yanpeng Zhang https://orcid.org/0000-0002-0954-7681

References

[1] Gisin N, Ribordy G, Tittel W and Zbinden H 2002 *Rev. Mod. Phys.* **74** 145–95
[2] Yamamoto Y and Haus H A 1986 *Rev. Mod. Phys.* **58** 1001–20
[3] Horodecki R, Horodecki P, Horodecki M and Horodecki K 2009 *Rev. Mod. Phys.* **81** 865–942
[4] Stevenson R M, Young R J, Atkinson P, Cooper K, Ritchie D A and Shields A J 2006 *Nature* **439** 179–82
[5] Ham B S, Shahriar M S and Hemmer P R 1999 *Opt. Lett.* **24** 86
[6] Utikal T, Eichhammer E, Petersen L, Renn A, Götzinger S and Sandoghdar V 2014 *Nat. Commun.* **5** 3627
[7] O'Brien J L 2007 Optical quantum computing *Science* **318** 1567–70
[8] Turukhin A V, Sudarshanam V S, Shahriar M S, Musser J A, Ham B S and Hemmer P R 2001 *Phys. Rev. Lett.* **88** 023602
[9] Beil F, Klein J, Nikoghosyan G and Halfmann T 2008 *J. Phys. B: At. Mol. Opt. Phys.* **41** 074001
[10] Wang H-H, Li A-J, Du D-M, Fan Y-F, Wang L, Kang Z-H, Jiang Y, Wu J-H and Gao J-Y 2008 *Appl. Phys. Lett.* **93** 221112
[11] Zhong T, Kindem J M, Miyazono E and Faraon A 2015 *Nat. Commun.* **6** 8206
[12] Vered R Z, Shaked Y, Ben-Or Y, Rosenbluh M and Pe'er A 2015 *Phys. Rev. Lett.* **114** 063902
[13] Qin Z, Cao L, Wang H, Marino A M, Zhang W and Jing J 2014 *Phys. Rev. Lett.* **113** 023602
[14] Liu C, Wang Y, Liu J, Zheng L, Su L and Xu J 2011 *Appl. Opt.* **50** 3229
[15] Ham B S, Hemmer P R and Shahriar M S 1997 *Opt. Commun.* **144** 227–30
[16] Fernandez-Gonzalvo X, Chen Y H, Yin C, Rogge S and Longdell J J 2015 *Phys. Rev.* A **92** 1–8
[17] Balić V, Braje D A, Kolchin P, Yin G Y and Harris S E 2005 *Phys. Rev. Lett.* **94** 183601
[18] Sheng Y-B, Zhou L, Zhao S-M and Zheng B-Y 2012 *Phys. Rev.* A **85** 012307
[19] Zhang Y, Zhang D, Zhang H, Tang H, Cheng L, Liu R and Zhang Y 2016 *Laser Phys. Lett.* **13** 115201
[20] Li C, Wang L, Yang C, Jiang T, Imran M, Ahmed I, Xiao M and Zhang Y 2015 *RSC Adv.* **5** 39449–54
[21] Chen H X, Qin M Z, Zhang Y Q, Zhang X, Wen F, Wen J M and Zhang Y P 2014 *Laser Phys. Lett.* **11** 045201
[22] Wu H and Xiao M 2009 *Phys. Rev.* A **80** 063415
[23] Clauser J F 1974 *Phys. Rev.* D **9** 853–60
[24] Boyer V, Marino A M, Pooser R C and Lett P D 2008 *Science* **321** 544–7